applied sciences

MDPI

Article

Optimal Generation Start-Up Methodology for Power System Restoration Considering Conventional and Non-Conventional Renewable Energy Sources

Ricardo Andrés Pardo-Martínez [1,2], Jesús M. López-Lezama [1,*] and Nicolás Muñoz-Galeano [1]

[1] Research Group on Efficient Energy Management (GIMEL), Departamento de Ingeniería Eléctrica, Universidad de Antioquia (UdeA), Medellín 050010, Colombia; ricardo.pardo@udea.edu.co (R.A.P.-M.); nicolas.munoz@udea.edu.co (N.M.-G.)

[2] XM, Expertos en Mercados, Calle 12 Sur 18-168, Medellín 050022, Colombia

* Correspondence: jmaria.lopez@udea.edu.co

Abstract: Power system restoration must be accomplished as soon as possible after a blackout. In this process, available black-start (BS) units are used to provide cranking power to non-black-start (NBS) units so as to maximize the overall power system generation capacity. This procedure is known as the generation start-up problem, which is intrinsically combinatorial with complex non-linear constraints. This paper presents a new mixed integer linear programming (MILP) formulation for the generation start-up problem that integrates non-conventional renewable energy sources (NCRES) and battery energy storage systems (BESS). The main objective consists of determining an initial starting sequence for both BS and NBS units that would maximize the generation capacity of the system while meeting the non-served demand of the network. The nature of the proposed model leads to global optimal solutions, clearly outperforming heuristic and enumerative approaches, since the latter may take higher computational time while the former do not guarantee global optimal solutions. Several tests were carried out on the IEEE 39-bus test system considering BESS as well as wind and solar generation. The results showed the positive impact of NCRES in the restoration processes and evidenced the effectiveness and applicability of the proposed approach. It was found that including NCRES and BESS in the restoration process allows a reduction of 24.4% of the objective function compared to the classical restoration without these technologies.

Keywords: power system restoration; non-conventional renewable energy sources (NCRES); battery energy storage systems (BESS); black-start (BS); non-black-start (NBS); mixed integer linear programming (MILP)

check for updates

Citation: Pardo-Martínez, R.A.; López-Lezama, J.M.; Muñoz-Galeano, N. Optimal Generation Start-Up Methodology for Power System Restoration Considering Conventional and Non-Conventional Renewable Energy Sources. *Appl. Sci.* **2021**, *11*, 8246. https://doi.org/10.3390/app11178246

Academic Editor: Tomonobu Senjyu

Received: 1 July 2021
Accepted: 31 August 2021
Published: 6 September 2021

1. Introduction

The development of new technologies in power systems has led to more flexible and robust networks; nevertheless, the risk of a total power system blackout is still present. There are many situations that may cause power system blackouts such as transmission line tripping and overloading, failure of protection or control systems, voltage collapse and cyber attacks, among others [1]. Power system blackouts around the world, such as the 2003 North American blackout [2], 2006 European blackout [3], 2007 Colombian blackout [4], and 2013 Indian blackout [5] bring about great economic losses and may even endanger human lives [6]. Despite all efforts to prevent their occurrence, the risk of blackouts is inherent in complex power systems; therefore, counting with proper methodologies for system restoration is of paramount importance for power system planners and operators.

Electric power generation units are divided in two groups based on the required power to start up: BS units that can start with their own internal resources (which include hydro, diesel, and gas turbine units [7]), and NBS units that require external power sources for starting up [8]. The restoration of a power system begins with BS units, which provide the initial power necessary to start up the NBS units. At the same time, as new units are started up increasing the availability of power generation, the loads are reconnected to maintain the stability of the power system [9].

Power system restoration following a blackout is one of the most important tasks of power system operators at control centers. It is a complex process aimed at setting the system back to normal operation after an extensive outage. The experience learned from historical blackouts has demonstrated that an efficient power system restoration plan is of utmost importance [10]. Generally, a common approach to the restoration process consists of three phases: the start-up of generators, the re-energizing of the network, and the restoration of load. The common thread linking each of these stages is the generation availability at each restorative stage.

Researchers have worked towards new models and solutions to solve the optimal generation start-up sequence, which is the most important feature of the restoration problem. In [11], an ant colony optimization algorithm is proposed to determine the optimal generation start-up sequence during bulk power system restoration. In this case, the authors intend to maximize the system generation capacity over the restoration period considering the characteristics of different types of generation units and system constraints. In [12], a firefly optimization algorithm is implemented to find the optimal starting generation sequence that minimizes the overall restoration time of a power system. In [13], a genetic algorithm is used to obtain the optimal unit restoration sequence taking into account a decreasing trend of unit start-up efficiency. In [14], a backtracking algorithm is adopted to determine the best unit restarting sequence considering a two-layer restoration process. The aforementioned heuristic methods provide good solutions to the restoration problem; nonetheless, their computational complexity require more time than the available during the restoration process; also, the achievement of a global optimal solution is not guaranteed. On the other hand, knowledge-based system approaches such as the ones presented in [15,16] require special software tools for which the maintenance and support are often impractical for the power industry. Some conventional optimization methods have also been proposed to provide more accurate solutions to the optimal restoration problem of power systems. In [17], the authors solve the generation start-up sequence and load pick up through a branch-and-bound and interior point method to provide an optimal skeleton-network restoration. In [18], the authors propose the integration of microgrids within the back-start optimization problem. In this case, the uncertainties of the microgrid black-start resources are modeled by discretizing the probability distribution of the forecast errors. A mixed integer linear programming model is implemented to solve the generator start-up sequence. In [19], the authors propose a distributed black-start optimization method for global transmission and distribution networks. In this case, the global black-start optimization problem is divided in several sub-problems in transmission and distribution networks taking advantage of distributed generation. Other methodologies to solve the optimal stat-up sequence for system restoration include bilevel optimization [9], dynamic programming [20], mixed-integer linear programming [21], Lagrangian relaxation [22], and Benders decomposition [23].

Depending on the structure and characteristics of the power system, its restoration process may be different. On the one hand, in power systems with a high number of BS units, the power system is restored quickly due to the availability of sufficient initial power resources. On the other hand, in power systems with a limited number of BS units, the system restoration results are more complicated and time consuming. In this research, the restoration of power systems with a limited number of BS resources and available renewable power plants is discussed. The main contributions of this paper are twofold: (i) it provides a novel mixed integer linear programming approach to solve the optimal generation start-up power system restoration problem, and (ii) it considers the effect of non-conventional renewable energy sources (NCRES) within the restoration process.

Table 1 presents a brief account of several methodologies applied to the optimal generation start-up problem, where CG and MIQP stand for conventional generation and mixed integer quadratic programming, respectively. Note that the proposed approach is the only one that simultaneously considers CG, NCERS, and BESS. It is worth mentioning that BESS have already been considered in start-up methodologies such as in [24,25]; nonetheless, in these works the authors integrate BESS in the black-start problem from the standpoint of the expansion planning aimed at improving the system resiliency, and not from an operative perspective, as carried out in this paper.

Table 1. Optimal generation start-up methodologies.

Reference	Year	Methodology	CG	NCRES	BESS
[16]	2011	Fuzzy logic	X		
[14]	2012	Lexicographic optimization	X		
[10]	2014	Pareto search through NSGA-II	X		
[26]	2014	Heuristic strategies	X	X	
[27]	2014	Spanning tree search	X	X	
[12]	2015	Firefly algorithm	X	X	
[22]	2015	Lagrangian relaxation	X	X	
[20]	2017	Dynamic programming	X	X	
[18]	2018	MILP	X	X	
[17]	2019	Branch-and-bound	X		
[19]	2021	MIQP	X	X	
This paper	2021	MILP	X	X	X

This paper is organized as follows: Section 1 provides an introduction and literature review regarding the power system restoration problem. Section 2 describes the conventional and non-conventional generation start-up strategy. Section 3 displays the proposed mathematical formulation for the generation start-up problem. Section 4 offers the test and results performed on the IEEE-39 RTS test system evidencing the impact of considering NCRES and battery energy storage systems (BESS) in the restoration process; finally, Section 5 presents the conclusions.

2. Conventional and Non-Conventional Generation Start-Up Strategies

NCRES have significantly increased their presence in electric power systems; therefore, such technologies are more frequently integrated into power system planning and operation studies [28]. This section presents the main guidelines that must be considered when integrating NCRES into a restoration process.

- The objective of the methodology is to maximize the generation capacity of the system and minimize the non supplied energy in a blackout.
- Before starting the restoration process, a preliminary analysis should be carried out to identify the cause of the event as well as available and unavailable resources. Knowing this before starting the system restoration will make the process more effective.
- BS units are the first ones to enter the system. For these units, a start-up time equal to zero is considered in the model.
- BESS will serve as BS units and will aim at bringing cranking power to NBS units to accelerate their start-up. They will also contribute to the normalization of priority loads.
- A priority order must be considered when performing the service restoration. There are priority loads that must be attended first such as control centers, aqueducts, hospitals, and substations.

- NCRES are considered in this methodology as NBS units; however, due to the benefits of their control systems; their power rise time is considered to be much less than that of conventional generators. With this fact, it will be assumed that the start-up of renewable resources are of the step type.
- Conventional NBS units can be started if they meet minimum or maximum start-up times, depending on the technical characteristics of the unit. Further, they require minimum starting power; that is to say, generation units will only be able to start until there is a power in the system equal to or greater than their declared starting power.
- NBS units based on NCRES can start if they meet the following conditions:
  - Minimum starting power.
  - Frequency stability to events in the restoration process. The starting of NCRES takes place when there is minimal inertia in the system. This inertia value is determined by the system operator through planning studies such as TMR (transmission must run). TMR is an indicator that determines the minimum generation required that must be online and operating at specific levels. This generation compensates for the lack of transmission networks in relation to the demand that is being restored.
  - Minimum firm generation. To comply with this condition, it is necessary to have adjusted historical and forecast data for both wind and solar generation production and the primary resource associated with these generation sources. These data serve as input to the proposed methodology to calculate average values and generation probabilities from the data series.
- PV and wind NCRES will have as their main function within the restoration process to accelerate the demand meeting process and compensate the load-generation imbalances while gaining stability in the system.

A MILP model is built based on the proposed methodology as illustrated in Figure 1. At first glance, it might be inferred that NCRES units should be the first ones to be started, prioritizing the fastest units to speed up the restoration process; however, there are more factors that affect the start-up process such as the stochastic characteristics of solar and wind resources and also the lack of inertia of the system. In consequence, an optimization process is required to find the best solution that ensures a fast but secure restoration. As illustrated in Figure 2, prioritizing the connection of a NCRES unit with maximum power output does not guarantee to achieve an optimal solution to the restoration problem [20]. With the generation profiles available in Figure 2 and assuming that at t_0 it is determined which unit should be connected to the system; it can be thought that PW_1 should be the first unit to be connected, because it has the maximum power output; however, at t_1, the power output of PW_1 drops drastically. In this case, the sudden decrease in PW_1 output will limit the ability to restore demand at later stages of the process; therefore, another unit must be considered to begin the restoration process even if it features lower power output.

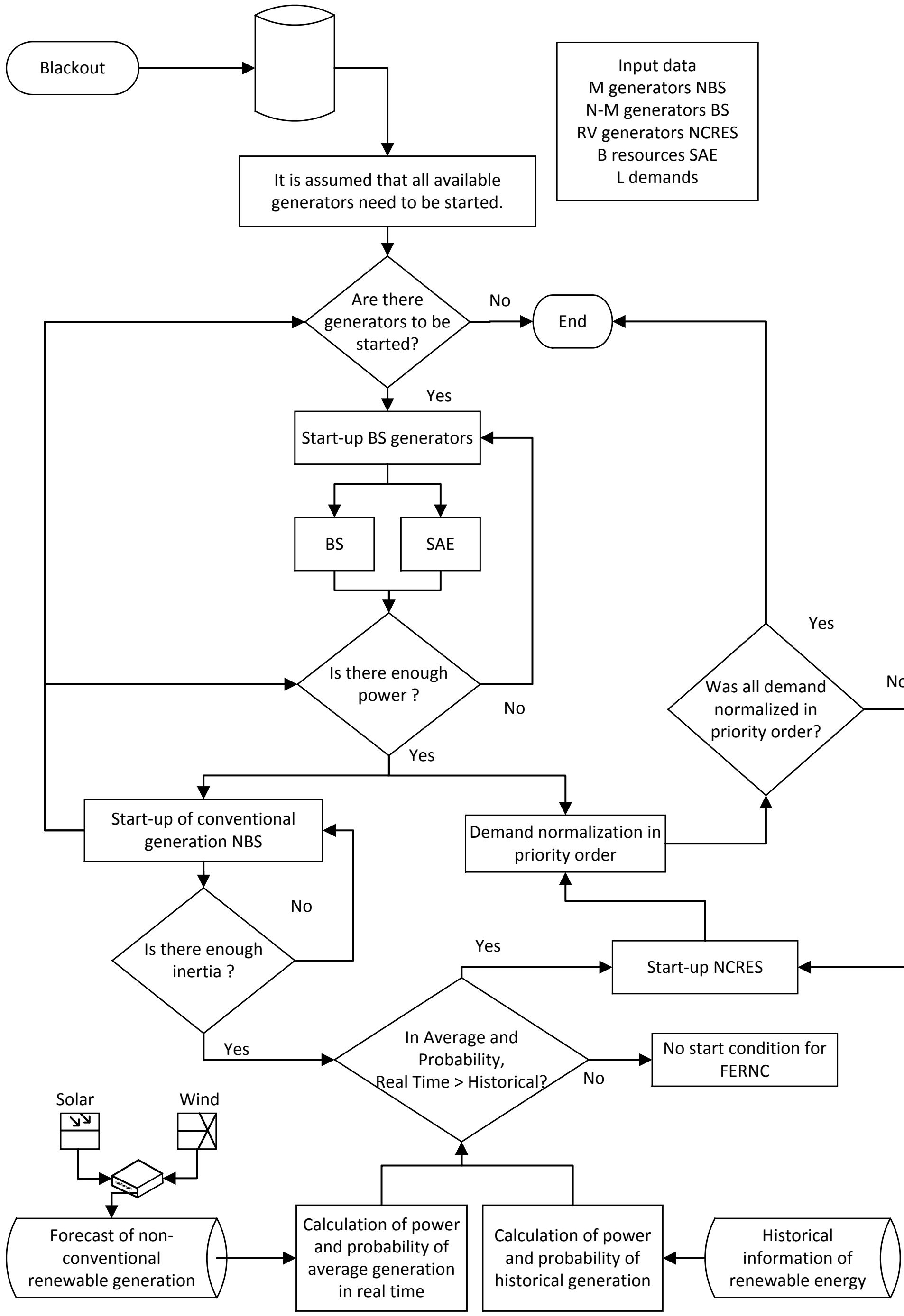

Figure 1. Flow chart of the conventional and non-conventional generation start-up methodology.

This research work opens a new field in the modeling of the restorative state of electric power systems with NCRES and BESS. Among the areas that can be covered in order to continue with this research and overcome current limitations, the following have been identified:

- The restoration process is a complex problem that must be observed from different aspects: generation, transmission, distribution, and demand. This research work covers directly the generation and indirectly the demand aspects. In this sense, this research work presents a methodology that provides the first signal or iteration of the restoration route, but does not provide the full route, which must also include the transmission network.

- To make the problem more complete, transmission and distribution networks should be added to the methodology. This research takes into account only the generation part and although it provides a good starting point, it is not the definitive scenario. Within the restoration process, constraints associated with the normalization of the network must be taken into account, such as the number of maneuvers to be performed and the conditions of voltage and frequency stability. For example, the following constraints can be considered: the Ferranti effect when long lines are to be normalized, the normalization of radial networks in the first instance, not energizing lines in parallel until a certain degree of network robustness is reached, energizing transformers in parallel only when 50 % of the chargeability of one of the transformers is reached, etc.
- The behavior of the variability and uncertainty of the primary FERNC generation resource should be further analyzed. It is recommended to model these variables in an optimization problem under uncertainty.
- New constraints may be included in the methodology if the full network model is used. Voltage, stability, and operation problems of transformer tap changers, as well as system losses, could also be considered from this approach.

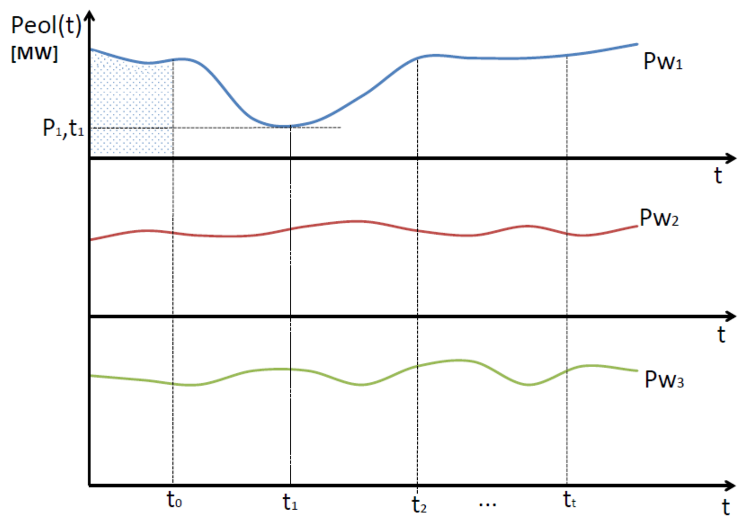

Figure 2. Simplified scenario of NCRES participation in a restoration process.

3. Problem Formulation

Metaheuristic approaches such as the ones proposed in [12,14,26] applied to the restoration problem are suitable to tackle non-convex models. Nonetheless, for MILP problems such as the one approach in this paper, classical mathematical approaches are the best alternative, since, as opposed to metheuristic techniques they guarantee a global optimal solution.

3.1. Objective Function

In the development of this research the objective functions defined in [29–31] are taken as a guide. The direct objective is to maximize the system's overall generation capacity $Egen_{sys}$ during a restoration period. Further, the indirect objective is to minimize the unserved load energy ENS_{sys} of the power system. In Equation (1), $Egen_{sys}$ is the sum of MW generation capabilities over all units in the power system minus the start-up power requirements. E_{igen} and E_{jstart} are the MW capability of generator i and start-up requirement of NBS generator j, respectively. Further, N and M are the number of BS and NBS units, respectively.

$$Egen_{sys} = \sum_{i=1}^{N} E_{igen} - \sum_{j=1}^{M} E_{jstart} \quad (1)$$

Equation (1) can be expressed in terms of BS and NBS generators as indicated in Equation (2). In this case, k and j are the indexes of BS and NBS generators, respectively; while N and M are the total number of generators and NBS generators, respectively.

$$Egen_{sys} = \left[\sum_{k=1}^{N-M} E_{kgen} + \sum_{j=1}^{M} E_{jgen} \right] - \sum_{j=1}^{M} E_{jstart} \tag{2}$$

Figure 3 characterizes the capacity of BS and NBS units and the starting requirements of an NBS generator. The MW capability of each generator, over the system restoration horizon, can be calculated using the area under the curve of Figure 3a. Similarly, the start-up requirement for each NBS generator is represented using the area under the curve of Figure 3b. The MW capacity is obtained using Equation (3). In this case, P_{imax} in [MW] is the maximum generator active power output, P_{jstart} in [MW] is the start-up power requirement for generator j, R_{ri} in [MW/h] is the generator ramping rate, t_{istart} in [h] and t_{jstart} in [h] are the restoration times of the ith and jth generators, respectively, and T is the total restoration time in [h].

$$\begin{aligned} Egen_{sys} &= \sum_{i=1}^{N} E_{igen} - \sum_{j=1}^{M} E_{jstart} \\ &= \sum_{i=1}^{N} \left\{ \frac{1}{2} P_{imax} \frac{P_{imax}}{R_{ri}} + P_{imax} \left[T - \left(t_{istart} + T_{ictp} + \frac{P_{imax}}{R_{ri}} \right) \right] \right\} - \sum_{j=1}^{M} P_{jstart} (T - t_{jstart}) \\ &= \left\{ \sum_{i=1}^{N} \left[\frac{(P_{imax})^2}{2R_{ri}} + P_{imax} \left(T - T_{ictp} - \frac{P_{imax}}{R_{ri}} \right) \right] - \sum_{j=1}^{M} P_{jstart} T \right\} - \\ &\left(\sum_{i=1}^{N} P_{imax} t_{istart} - \sum_{j=1}^{M} P_{jstart} t_{jstart} \right) \end{aligned} \tag{3}$$

Simplifying Equation (3) as in [29] leads to Equation (4) where P_{jmax} is the maximum capability of NBS units, P_{jstart} is the start-up power requirement constraints of NBS units, and t_{jstart} is their corresponding start times.

$$E_{sys} = \sum_{j=1}^{M} (P_{jmax} - P_{jstart}) t_{jstart} \tag{4}$$

The proposed objective function can be expressed as indicated in Equation (5), which also considers the minimization of the unserved load energy. In this case, the factor $(P_{Lsys} - P_{Lcl})\Delta t$ is the unserved load energy; where P_{Lsys} in [MW] is the total power demand of the system and P_{Lcl} in [MW] is the total restored load at time Δt in [h].

$$minimize \sum_{j=1}^{M} (P_{jmax} - P_{jstart}) t_{jstart} + \sum_{t=1}^{T} \sum_{l=1}^{L} (P_{Lsys} - P_{Lcl}) \Delta t \tag{5}$$

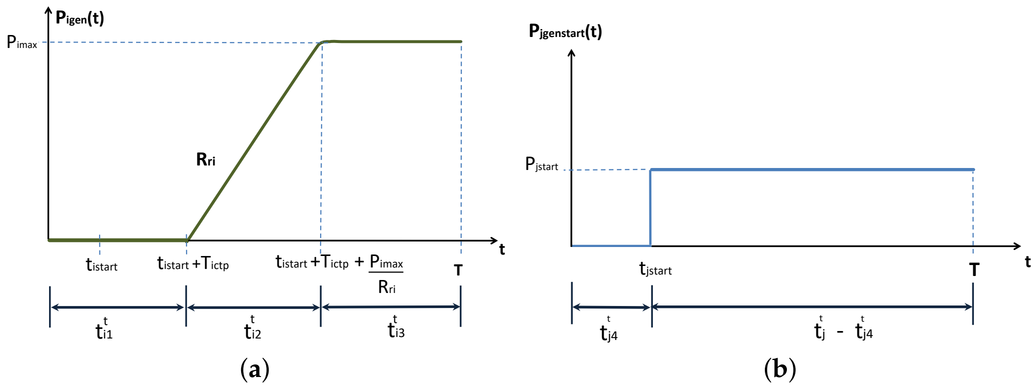

Figure 3. Characterization of conventional generators: (**a**) capacity curves for BS and NBS units; (**b**) starting curve of an NBS generator.

3.2. Constraints

The following constraints are considered in the optimal generator start-up problem.

3.2.1. Critical Minimum and Maximum Intervals

If an NBS unit does not start within a critical maximum time interval T_{cmax} in [h], the unit will not be available until after a considerable time delay. Further, an NBS unit with a critical minimum time interval constraint T_{cmin} in [h], cannot be restarted until this time expires. Equation (6) represents this critical time constraint.

$$
\begin{aligned}
t_{jstart} &\geq T_{jcmin} \\
t_{jstart} &\leq T_{jcmax}
\end{aligned}
\tag{6}
$$

3.2.2. Start-Up Power Requirement

This constraint is represented by Equation (7), where $P_{igen(t)}$ in [MW] is the generation capability function of generator i, $P_{istart(t)}$ in [MW] is the start-up power requirement function of NBS generator i, RV is the number of NCRES generators, and $P_{rvstart(t)}$ in [MW] is the start-up requirement function of the NCRES generators.

$$
\sum_{i=1}^{N} P_{igen}(t) - \sum_{j=1}^{M} P_{istart}(t) - \sum_{rv=1}^{RV} P_{rvstart}(t) \geq 0, \quad t = 1, 2, \ldots, T \tag{7}
$$

Equations (1)–(7) represent a nonlinear combinatorial optimization problem. The proposed formulation that corresponds to a MILP problem relies on a series of transformations that are described in the following paragraphs.

Initially, it is necessary to introduce new decision variables for defining the generator capability function of Figure 3a, which corresponds to a piecewise linear function. Note that Figure 3a shows the point $(t_{istart} + t_{ictp}, 0)$ at which the generator begins to ramp up. The point $(t_{istart} + t_{ictp} + P_{imax}/Rri, P_{imax})$, at which the generator reaches its maximum generation capability separates the curve into three segments: t_{i1}^{t}, t_{i2}^{t}, and t_{i3}^{t}. Here, w_{i1}^{t} and w_{i2}^{t} are binary decision variables that restrict these three variables within the corresponding range. Equation (8) represents the piecewise generator capability function.

$$
\begin{aligned}
P_{igen}(t) &= R_{ri} \cdot t_{i2}^{t} \\
t &= t_{i1}^{t} + t_{i2}^{t} + t_{i3}^{t} \\
w_{i1}^{t}\left(t_{istart} + T_{ictp}\right) &\leq t_{i1}^{t} \leq t_{istart} + T_{ictp} \\
w_{i2}^{t}\frac{P_{imax}}{R_{ri}} &\leq t_{i2}^{t} \leq w_{i1}^{t}\frac{P_{imax}}{R_{ri}} \\
0 \leq t_{i3}^{t} &\leq w_{i2}^{t}\left(T - t_{istart} - T_{ictp} - \frac{P_{imax}}{R_{ri}}\right) \\
w_{i2}^{t} &\leq w_{i1}^{t} \\
w_{i2}^{t}, w_{i1}^{t} &\in \{0,1\} \\
t_{i1}^{t}, t_{i2}^{t}, t_{i3}^{t} &\in (0,1,2,\ldots,T)
\end{aligned} \tag{8}
$$

In Equation (8), the start-up time of BS units is zero ($t_{kstart} = 0$). In consequence, Equation (8) can be reformulated as in Equation (9).

$$
\begin{aligned}
P_{igen}(t) &= R_{ri} \cdot t_{i2}^{t} \\
t &= t_{i1}^{t} + t_{i2}^{t} + t_{i3}^{t} \\
w_{k1}^{t} T_{kctp} &\leq t_{k1}^{t} \leq T_{kctp} \\
w_{j1}^{t}\left(t_{jstart} + T_{jctp}\right) &\leq t_{j1}^{t} \leq t_{jstart} + T_{jctp} \\
w_{i2}^{t}\frac{P_{imax}}{R_{ri}} &\leq t_{i2}^{t} \leq w_{i1}^{t}\frac{P_{imax}}{R_{ri}} \\
0 \leq t_{k3}^{t} &\leq w_{k2}^{t}\left(T - T_{kctp} - \frac{P_{kmax}}{R_{rk}}\right) \\
0 \leq t_{j3}^{t} &\leq w_{j2}^{t}\left(T - t_{jstart} - T_{jctp} - \frac{P_{jmax}}{R_{rj}}\right) \\
w_{i2}^{t} &\leq w_{i1}^{t} \\
w_{i2}^{t}, w_{i1}^{t} &\in \{0,1\} \\
t_{i1}^{t}, t_{i2}^{t}, t_{i3}^{t} &\in (0,1,2,\ldots,T)
\end{aligned} \tag{9}
$$

Equation (9) corresponds to a non-linear constraint. Note that there is a product of one binary decision variable (w_{j1}^{t}) and one integer decision variable (t_{jstart}). Equation (9) can be transformed into linear expressions by using Equation (10). In this case, $BigM$ is an upper positive bound of y_{jh}^{t} and w_{jh}^{t} is its associated binary variable. If $w_{jh}^{t} = 1$, then the constraint is relaxed and is met by default $y_{jh}^{t} \leq BigM$. Otherwise; if $w_{jh}^{t} = 0$, then $y_{jh}^{t} \leq 0$. So this constraint allows modeling the proposition $w_{jh}^{t} = 0 \Longrightarrow y_{jh}^{t} \leq 0$. Furthermore, if $y_{jh}^{t} > 0$ then $w_{jh}^{t} = 1$. If $y_{jh}^{t} \leq 0$ the constraint does not imply anything $y_{jh}^{t} > 0 \Longrightarrow w_{jh}^{t} = 1$.

$$
\begin{aligned}
y_{jh}^{t} &= w_{jh}^{t} \cdot t_{jstart} \\
y_{jh}^{t} &\geq 0 \\
y_{jh}^{t} &\leq BigM \cdot w_{jh}^{t} \\
-t_{jstart} + y_{jh}^{t} &\leq 0 \\
t_{jstart} - y_{jh}^{t} + BigM \cdot w_{jh}^{t} &\leq BigM \\
t_{jstart} &\leq BigM
\end{aligned} \tag{10}
$$

By replacing (10) in (9), Equation (11) is obtained.

$$
\begin{aligned}
P_{igen}(t) &= R_{ri} \cdot t_{i2}^t \\
t &= t_{i1}^t + t_{i2}^t + t_{i3}^t \\
w_{k1}^t T_{kctp} &\leq t_{k1}^t \leq T_{kctp} \\
y_{j1}^t + w_{j1}^t T_{jctp} &\leq t_{j1}^t \leq t_{jstart} + T_{jctp} \\
w_{i2}^t \frac{P_{imax}}{R_{ri}} &\leq t_{i2}^t \leq w_{i1}^t \frac{P_{imax}}{R_{ri}} \\
0 &\leq t_{k3}^t \leq w_{k2}^t \left(T - T_{kctp} - \frac{P_{kmax}}{R_{rk}} \right) \\
0 &\leq t_{j3}^t \leq w_{j2}^t \left(T - T_{jctp} - \frac{P_{jmax}}{R_{rj}} \right) - y_{j2}^t \\
w_{i2}^t &\leq w_{i1}^t \\
y_{j1}^t &\geq 0 \\
y_{j2}^t &\geq 0 \\
y_{j1}^t &\leq BigM \cdot w_{j1}^t \\
y_{j2}^t &\leq BigM \cdot w_{j2}^t \\
-t_{jstart} + y_{j1}^t &\leq 0 \\
-t_{jstart} + y_{j2}^t &\leq 0 \\
t_{jstart} - y_{j1}^t + BigM \cdot w_{j1}^t &\leq BigM \\
t_{jstart} - y_{j2}^t + BigM \cdot w_{j2}^t &\leq BigM \\
t_{jstart} &\leq BigM \\
w_{i2}^t, w_{i1}^t &\in \{0, 1\} \\
t_{i1}^t, t_{i2}^t, t_{i3}^t &\in (0, 1, 2, \ldots, T)
\end{aligned} \tag{11}
$$

It is also necessary to introduce binary decision (w_{j3}^t) and linear decision (t_{j4}^t) variables for defining the generator start-up power function that corresponds to a step function. Figure 3b shows the point $(t_{istart}, 0)$, where an NBS generator receives the cranking power to be started up; the curve is separated into two segments: t_{j4}^t and $t_j^t - t_{j4}^t$. In this case, w_{j3}^t restricts these variables within the corresponding range. Equation (12) represents the generator capability function.

$$
\begin{aligned}
P_{jstart}(t) &= w_{j3}^t \cdot P_{jstart} \\
w_{j3}^t (t_{jstart} - 1) &\leq t_{j4}^t \leq t_{jstart} - 1 \\
w_{j3}^t &\leq t^t - t_{j4}^t \leq w_{j3}^t (T - t_{jstart} + 1)
\end{aligned} \tag{12}
$$

Due to the expression $w_{j3}^t \cdot t_{jstart}$ Equation (12) is a non-linear constraint. By applying a linear transformation of Equation (10), Equation (13) is obtained.

$$
\begin{aligned}
P_{jstart}(t) &= w_{j3}^t \cdot P_{jstart} \\
y_{j3}^t - w_{j3}^t &\leq t_{j4}^t \leq t_{jstart} - 1 \\
w_{j3}^t &\leq t^t - t_{j4}^t \leq w_{j3}^t (T + 1) - y_{j3}^t \\
y_{j3}^t &\geq 0 \\
y_{j3}^t &\leq BigM \cdot w_{j3}^t \\
-t_{jstart} + y_{j3}^t &\leq 0 \\
t_{jstart} - y_{j3}^t + BigM \cdot w_{j3}^t &\leq BigM
\end{aligned} \tag{13}
$$

Equations (11) and (13) allow rewriting Equation (7) as in (14).

$$\sum_{i=1}^{N} R_{ri} \cdot t_{i2}^{t} - \sum_{j=1}^{M} w_{j3}^{t} \cdot P_{istart} - \sum_{rv=1}^{RV} w_{rvst}^{t} \cdot P_{rvstart} \geq 0, \quad t = 1, 2, \ldots, T \tag{14}$$

3.2.3. Load Restoring

Load can only be restarted when the system can supply sufficient power (P_{sys}). In Figure 4, $P_{load(t)} in[MW]$ characterizes the load restoration function (step function), at $(t_{lrest}, 0)$, the load receives the power to be restored. In this case, t_{lrest} separates the curve into two segments: t_{l5}^{t} and $t_{l}^{t} - t_{l5}^{t}$, while w_{l4}^{t} is a binary variable that restricts these segments within the corresponding range. Equation (15) corresponds to the load restoring function. $P_{lc(t)}$ in [MW] is the value of restoring load at the time T.

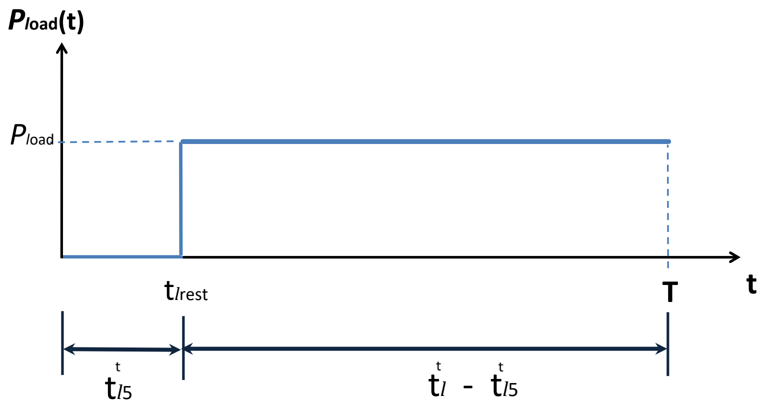

Figure 4. Step function of the load restoration.

$$\begin{aligned} P_{lc}(t) &= w_{l4}^{t} \cdot P_{lc} \\ w_{l4}^{t}(t_{lrest} - 1) &\leq t_{l5}^{t} \leq t_{lrest} - 1 \\ w_{l4}^{t} &\leq t^{t} - t_{l5}^{t} \leq w_{l4}^{t}(T - t_{lrest} + 1) \end{aligned} \tag{15}$$

Equation (15) introduces both binary and linear decision variables. Similarly, by implementing a linear transformation of Equation (10), Equation (16) is obtained.

$$\begin{aligned} P_{lc}(t) &= w_{l4}^{t} \cdot P_{lc} \\ y_{l4}^{t} - w_{l4}^{t} &\leq t_{l5}^{t} \leq t_{lrest} - 1 \\ w_{l4}^{t} &\leq t^{t} - t_{l5}^{t} \leq w_{l4}^{t}(T+1) - y_{l4}^{t} \\ y_{l4}^{t} &= w_{l4}^{t} \cdot t_{lrest} \\ y_{l4}^{t} &\geq 0 \\ y_{l4}^{t} &\leq BigM \cdot w_{l4}^{t} \\ -t_{lrest} + y_{l4}^{t} &\leq 0 \\ t_{lrest} - y_{l4}^{t} + BigM \cdot w_{l4}^{t} &\leq M \\ t_{lrest} &\leq BigM \end{aligned} \tag{16}$$

3.2.4. Demand Priority

Restoration of system demand must be performed in a prioritized way. In Equation (17), t_{lrest} in [h] models the attention of priority loads or substations that must be energized first, such as control centers, aqueducts, or hospitals.

$$t_{lrest} \leq t_{(l+1)rest} \tag{17}$$

3.2.5. Inertia Requirements

This restriction guarantees sufficient inertia in the system for the entry of NCRES in such a way that there is frequency stability in face of undesired events in the restoration process. Each generation resource that enters into synchronism contributes to the inertia of the system. Equation (18), indicates that the binary variable w_{rvH}^{t} must be activated as long as sufficient inertia $Hmin_{sys}$ in [h] is ensured in the system. H_k and H_j in $[h]$ are the inertia of BS and NBS generators.

$$\sum_{k=1}^{N-M} w_{k1}^{t} \cdot H_k + \sum_{j=1}^{M} w_{j3}^{t} \cdot H_j - \left(w_{rvH}^{t} \cdot Hmin_{sys}\right) \geq 0 \tag{18}$$

3.2.6. NCRES Generation Probability

Constraint (19) ensures the availability of NCRES due to the volatility of such generation. In this case, $\overline{P}_{rvforec}^{t}$ in MW is the average power calculated from the NCRES forecast in a time period t after the blackout; $p(v)_{rvforec}$ is the probability of how long the primary resource of NCRES generation will be above its average value according to the forecast data; $\overline{P}_{rvhistmed}$ in MW is the average power calculated from historical NCRES power data for one week previous to the blackout; $p(v)_{rvhist}$ is the probability of how long the primary resource of NCRES generation was above its average value according to historical data.

$$w_{rvprob}^{t} \cdot \left[\left(\overline{P}_{rvforec}^{t} \cdot p(v)_{rvforec}\right) - \left(\overline{P}_{rvhistmed} \cdot p(v)_{rvhist}\right)\right] \geq 0 \tag{19}$$

3.2.7. Characterization Curve of BESS

BESS are modeled as BS units; however, these elements have limited energy. The generalized BESS discharge curve is defined as a function of three segments as shown in Equation (20) and Figure 5.

Points $\left(T_{bON} + t_{bctp}, SOC_b\right)$ and $\left(T_{bON} + t_{bctp} + \frac{SOC_b}{\eta_{bSOC}}, SOC_{bmin}\right)$ divide the curve into segments t_{b1}^{t}, t_{b2}^{t} and t_{b3}^{t}. This representation permits the modeling of the behavior of BESS, from the start of the descent ramp until its minimum value. The start-up time of these resources is equal to zero ($t_{bON} = 0$) while Equation (20) characterizes the start-up of these resources. Here, SOC_b in [MW] is the initial state of charge BESS, $SOCmin_b$ in [MW] is the state of charge minimum of BESS, $SOCmax_b$ in [MW] is the state of charge maximum of BESS and η_s in [MW/h] is the ramping rate of BESS.

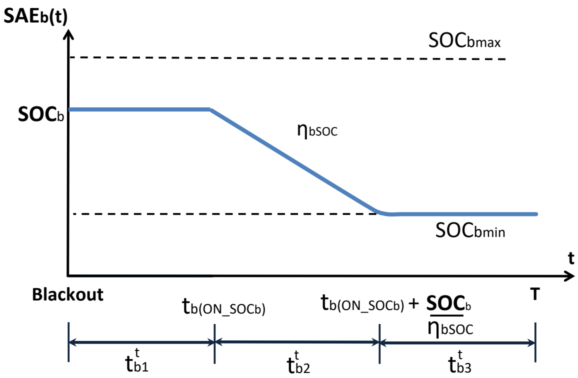

Figure 5. Generalized characterization curve of a restoring BESS.

$$
\begin{aligned}
SAE_b(t) &= w_{b1}^t \cdot SOC_b - \eta_{bSOC} \cdot t_{b2}^t \\
t &= t_{b1}^t + t_{b2}^t + t_{b3}^t \\
w_{b1}^t T_{bctp} &\leq t_{b1}^t \leq T_{bctp} \\
w_{b2}^t \frac{SOC_b}{\eta_{bSOC}} &\leq t_{b2}^t \leq w_{b1}^t \frac{SOC_b}{\eta_{bSOC}} \\
0 \leq t_{b3}^t &\leq w_{b2}^t \left(T - T_{bctp} - \frac{SOC_b}{\eta_{bSOC}} \right) \\
SOC_b - \eta_{bSOC} \cdot t_{b2}^t &\leq SOC_{bmin} \\
w_{b2}^t &\leq w_{b1}^t \\
w_{b2}^t, w_{b1}^t &\in \{0,1\} \\
t_{b1}^t, t_{b2}^t, t_{b3}^t &\in (0,1,2,\ldots,T)
\end{aligned} \tag{20}
$$

3.2.8. Load-Generation Balance

Equation (21) models the fact that demand is restored as long as there is enough power in the system.

$$
\sum_{k=1}^{N-M} R_{rk} \cdot t_{k2}^t + \sum_{j=1}^{M} R_{rj} \cdot t_{j2}^t + \sum_{b=1}^{B} \left[\left(w_{b1}^t \cdot SOC_b \right) - \left(\eta_{bSOC} \cdot t_{b2}^t \right) \right] + \sum_{rv=1}^{RV} vr_{2rv}^t \cdot P_{rvrt}^t \geq \sum_{l=1}^{L} w_{l4}^t \cdot P_{lc}, \quad t = 1,2,\ldots,T \tag{21}
$$

3.2.9. NCRES Start-Up Condition

Figure 6 characterizes NCRES generation capacity curve. The start-up of generation capacity curves type NCRES is modeled as a step function. This is because the response time of a NCRES generator is much faster than a conventional generator. Equation (22) characterizes the generation curve as a step piecewise linear function. Here, P_{rvrt}^t in [MW] represents NCRES forecast active power at the time T.

$$
\begin{aligned}
P_{rvrt}(t) &= vr_{2rv}^t \cdot P_{rvrt}^t \\
vr_{2rv}^t (t_{rvstart} - 1) &\leq t_{rv6}^t \leq t_{rvstart} - 1 \\
vr_{2rv}^t &\leq t^t - t_{rv6}^t \leq vr_{2rv}^t (T - t_{rvstart} + 1)
\end{aligned} \tag{22}
$$

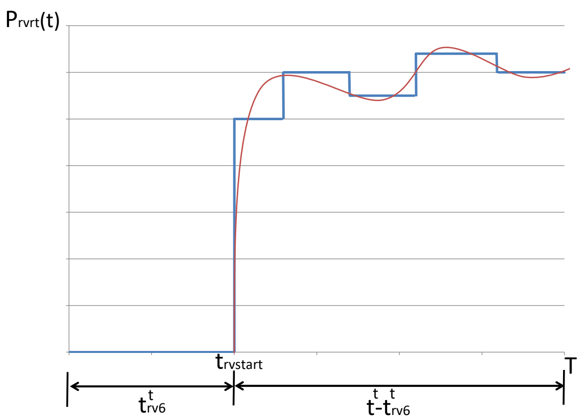

Figure 6. NCRES generation capacity curves.

Binary variable vr_{2rv}^t is used for starting NCRES and is activated when:

- There is enough power in the system to meet the minimum starting requirements of power units. This is represented using w^t_{rvst}.
- There is minimal inertia in the system to meet the frequency stability requirements. This is represented using w^t_{rvH}.
- There is sufficient primary resource conditions to guarantee firmness in the process. This is represented using w_{rvprob}.

Therefore, the activation of variable vr^t_{2rv} must simultaneously satisfy the three above mentioned conditions. This fact is modeled as the product of binary variables. The linearization is performed using Equation (23), which is explained in [32].

$$
\begin{aligned}
\delta_3 &= \delta_1 \cdot \delta_2 \\
\delta_3 &\leq \delta_1 \\
\delta_3 &\leq \delta_2 \\
\delta_1 + \delta_2 &\leq 1 + \delta_3 \\
\delta_1, \delta_2, \delta_3 &\in \{0,1\}
\end{aligned}
\tag{23}
$$

In this case, NCRES starting condition is fulfilled when the following inequalities are met:

$$
\begin{aligned}
vr^t_{1rv} &= w^t_{rvst} \cdot w^t_{rvH} \\
vr^t_{1rv} &\leq w^t_{rvst} \\
vr^t_{1rv} &\leq w^t_{rvH} \\
w^t_{rvst} + w^t_{rvH} &\leq 1 + vr^t_{1rv} \\
w^t_{rvst}, w^t_{rvH}, vr^t_{1rv} &\in \{0,1\} \\
vr^t_{2rv} &= w^t_{rvprob} \cdot vr^t_{1rv} \\
vr^t_{2rv} &\leq w^t_{rvprob} \\
vr^t_{2rv} &\leq vr^t_{1rv} \\
w^t_{rvprob} + vr^t_{1rv} &\leq 1 + vr^t_{2rv} \\
w^t_{rvprob}, w^t_{rvH}, vr^t_{2rv} &\in \{0,1\}
\end{aligned}
\tag{24}
$$

4. Tests and Results

Several tests were performed with the IEEE-39 RTS system for validating the proposed model. In the specialized literature, this test case does not present renewable generation; however, in [33] it is proposed to include six NCRES generators located at nodes 3, 5, 7, 16, 21, and 23. A laptop with an Intel (R) core (TM) i5-4200U @ 1.6 GHz 2.3 GHz processor, 6.00 GB of RAM, and a 64-bit operating system was used in all tests.

Although the system chosen to demonstrate the applicability of the proposed approach is relatively small, the scalability of the problem is straightforward. This is due to the fact that the model was implemented in GAMS (general algebraic modeling system) software. On the other hand, to reduce the computation time in real applications, several strategies can be explored such as parallelization or the use of computation equipment with higher performance.

4.1. Input Data

The IEEE-39 RTS system has 10 generators whose characteristics are presented in Table 2. An evaluation period of four hours with a granularity of 5 min is considered, which is equivalent to 55 periods of time. Table 3 shows the loads associated with the test system; the evaluated scenario considers a total blackout. For this case study, three solar and three wind-type generators were chosen, whose parameters are shown in Table 4.

Table 2. Generation parameters of the IEEE-39 RTS sytem.

i	Type	T_{ctp} [h]	T_{cmin} [h]	T_{cmax} [h]	Rr [MW/h]	P_{start} [MW]	P_{max} [MW]	$Inertia$ [s]
1	NBS	00:35	00:40	N/A	215	5.5	520	2.6
2	NBS	00:35	N/A	N/A	246	8	650	2.8
3	NBS	00:35	N/A	02:00	236	7	632	3.0
4	NBS	00:35	01:10	N/A	198	5	508	2.8
5	NBS	00:35	N/A	01:00	244	8	650	3.0
6	NBS	00:35	N/A	N/A	214	6	560	2.8
7	NBS	00:35	N/A	N/A	210	6	540	3.0
8	NBS	00:35	N/A	N/A	346	13.2	830	2.8
9	NBS	00:35	N/A	N/A	384	15	1000	3.0
10	BS	00:15	N/A	N/A	162	0	250	3.5

Table 3. Load parameters.

Node	Priority	Pl_{load} [MW]	Node	Priority	Pl_{load} [MW]
3	1	322	23	11	247
4	2	500	24	12	309
7	3	234	25	13	224
8	4	522	26	14	139
12	5	8	27	15	158
15	6	320	28	16	206
16	7	328	29	17	284
18	8	281	31	18	9
20	9	628	39	19	1104
21	10	274			

Table 4. Parameters of NCRES units.

rv	Type	$P_{rvstart}$ [MW]	P_{rvmax} [MW]	$\overline{P}_{rvforec}$	$p(v)_{rvforec}$	$\overline{P}_{rvhistmed}$	$p(v)_{rvhist}$
1	Wind 1	6	339.75	56.84	0.535	37.52	0.564
2	Wind 2	9	235.25	118.15	0.514	68.44	0.561
3	Wind 3	12	104.5	174.98	0.584	105.96	0.541
4	PV 1	6	132.65	78.17	0.486	38.76	0.549
5	PV 2	3	54.59	34.3	0.52	15.66	0.535
6	PV 3	5	98.17	57.67	0.469	29.33	0.28

The historical and forecast statistical data used to perform simulations were taken from different wind and PV generators operated by the TSO of Netherlands Elia Group [34]. The information selected to carry out the experimental tests corresponds to both the historical data series of 8 March 2020 from 00:00 to 08:30 h of 22 March 2020 with a granularity of 15 min; as well as the solar and PV generation prediction series for 22 March from 08:30 a.m. to 1:00 p.m. with a granularity of 5 min. These data are the input to the model illustrated in Figure 7. The parameters of BESS are presented in Table 5, where *b* stands for battery.

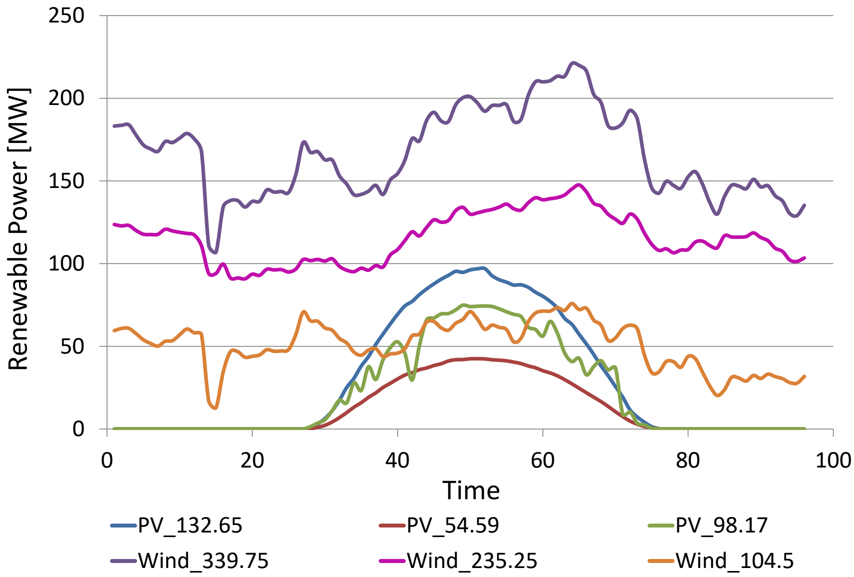

Figure 7. Renewable resources output power data.

Table 5. Parameters of BESS.

b	T_{bctp}	η_b [MW/ut]	SOC_B	P^t_{bstart}
1	1	0.5	30	0
2	1	1	20	0

The proposed optimization model was implemented under three scenarios: (1) only conventional generation, (2) NCRES and conventional generation, and (3) all technologies (conventional generation, NCRES, and BESS).

4.2. General Results

Table 6 presents the general results for the analyzed scenarios. After running the optimization model with the first scenario, an objective function of 227278.4 [MW/h] was obtained in a time of 27.16 [s]. In the second scenario, that considers the effect of NCRES, the objective function decreased 10.37% compared to the first scenario. When all available resources are integrated (third scenario), the objective function decreases by 27.4% compared to the first scenario. Note that including all technologies (NCRES and BESS apart from conventional generation) require more computing time and a higher number of iterations; nonetheless a better objective function is obtained.

Table 6. Objective function of the restoration process with and without NCRES and BESS.

Parameter	Conventional	NCRES	All Technologies
Objective Function Value [MW/h]	227,278.4	203,703.4	165,002.4
Execution time [s]	27.16	52.03	88.17
Iterations	145,447	154,646	327,239

Figure 8 shows the added generation profiles of the system for each of the three scenarios under consideration. As new types of resources are included, the total value of energy available in the system increases. Note that the greatest benefit is achieved when all technologies are involved in the restoration process.

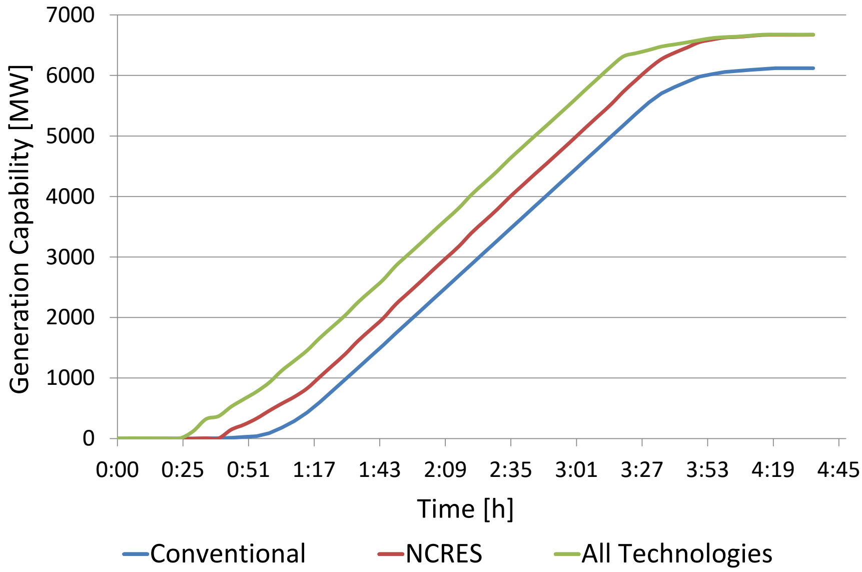

Figure 8. Generation available in the system for all scenarios.

4.3. *Comparison with Other Methodologies*

A comparison of the optimization model developed in this paper with other methodologies presented in the specialized literature is presented in this section. Table 7 shows, for different optimization techniques, the computational time and whether or not the global optimum was reached in the restoration process of the IEEE-39 RST test system with conventional generation. It can be observed that the methodology developed in this paper allows achieving a global optimal solution with a satisfactory computational time. It is worth mentioning that a comparison of the complete methodology integrating NCRES and BESS is not possible to carry out since to the best of the authors knowledge there are no other methodologies that simultaneously integrate this two resources within the optimal restoration process (see Table 1). On the other hand, a comparison regarding the execution time would not be fare, since the results were obtained with different computers. The enumeration algorithm was processed on a Core i3 computer @ 2.53 GHz. The two-step algorithm does not refer to the characteristics of the test computer, and the proposed methodology was performed on a computer with Intel(R) core(TM) i5-4200U @ 1.6 GHz 2.3 GHz.

Table 7. Comparison with other methods.

Algorithm	Global Solution?	Computation Time [hh:mm:ss]	Reference
Enumeration	Yes	01:53:00	[30]
Two-step algorithm	No	00:04:00	[31]
MILP	Yes	00:01:29	This paper

4.4. *Progression of Unserved Energy in the System*

Figure 9 shows that as NCRES and BESS resources are integrated; the unserved demand decreases. Despite the fact that NCRES do not participate directly in the starting of NBS units, they allow speeding up the process of restoring demand guaranteeing a faster response for the load-generation balance.

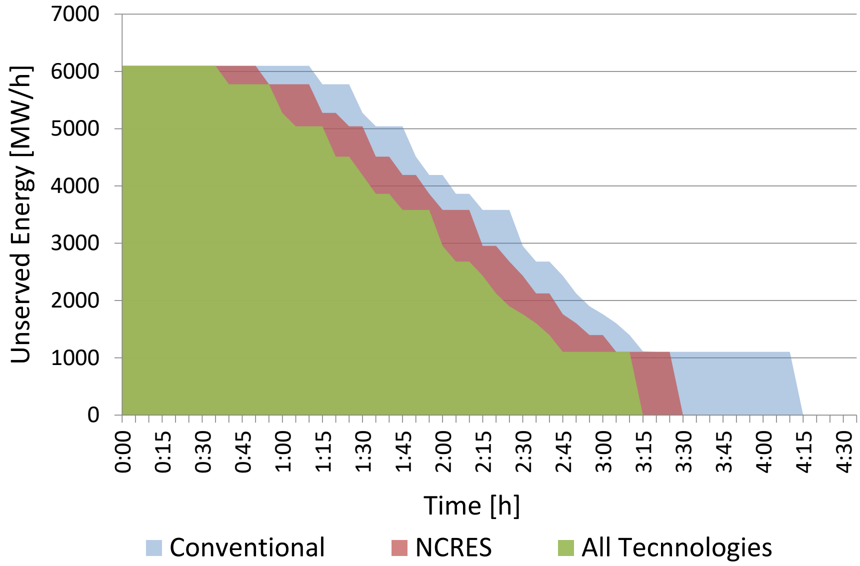

Figure 9. Unserved energy for different scenarios.

Figure 9 shows that with the integration of NCRES the demand recovery time decreases in 45 min (it would take up to 4 h 15 min if only conventional generation is used), which is equivalent to 17.6% of the total time used in scenario 1. By implementing all the resources in the system, this time decreases 1 h, which is equivalent to 23.52% of the total time in scenario 1. The unserved energy is correlated proportionally to the reestablishment times of unserved demand. This means that the unserved energy decreases as the demand recovery times shorten. Figure 10 shows the demand restoration progression times in the system where the advantage of having a mixed of NCRES and BESS is also evident.

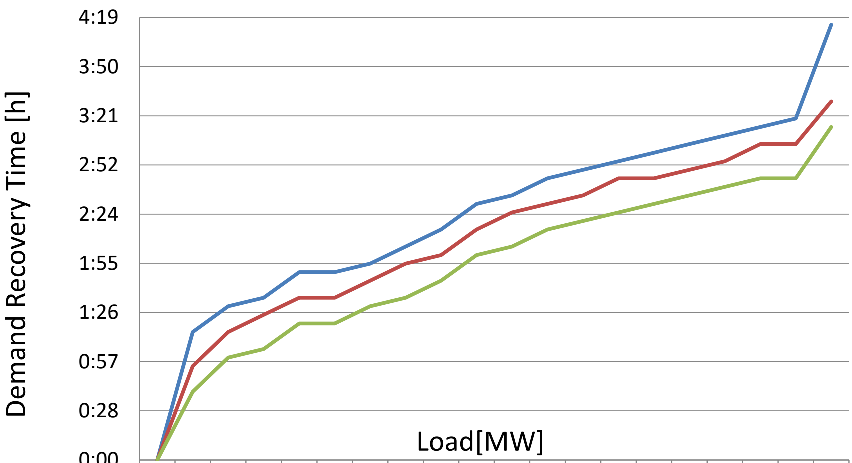

	0	322	500	234	522	8	320	329	281	628	274	247	309	224	139	158	206	284	9	1104
Conventional	0:00	1:15	1:30	1:35	1:50	1:50	1:55	2:05	2:15	2:30	2:35	2:45	2:50	2:55	3:00	3:05	3:10	3:15	3:20	4:15
NCRES	0:00	0:55	1:15	1:25	1:35	1:35	1:45	1:55	2:00	2:15	2:25	2:30	2:35	2:45	2:45	2:50	2:55	3:05	3:05	3:30
All Technologies	0:00	0:40	1:00	1:05	1:20	1:20	1:30	1:35	1:45	2:00	2:05	2:15	2:20	2:25	2:30	2:35	2:40	2:45	2:45	3:15

Figure 10. Demand recovery times.

4.5. Start-Up Times of Generation Units

Regarding the start-up times of the generation units, Figure 11 shows that scenarios 1 and 2 present the same time. This is because in the proposed approach NCRES are considered as NBS resources whose main function is to restore demand and guarantee the load-generation balance.

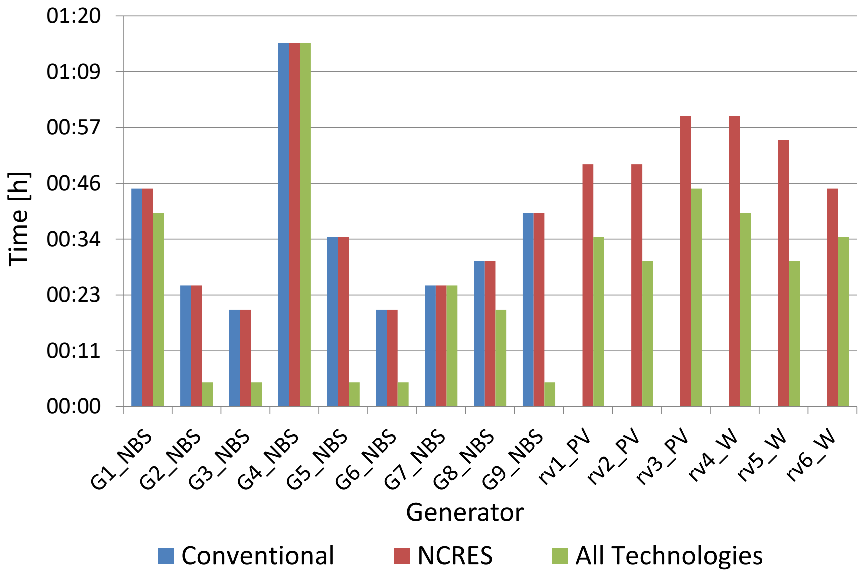

Figure 11. Generators start-up times.

Nonetheless, an evident improvement in the start-up process occurs when BESS units are added. Figure 12 shows the discharge power of the batteries considered in the test system. Note that there are two slopes in the discharge of these resources. According to Table 5, the first slope, until 01:45 [Hrs], represents the discharge of battery $b = 2$; while the second slope, until 04:19 [Hrs], represents the discharge of battery $b = 1$.

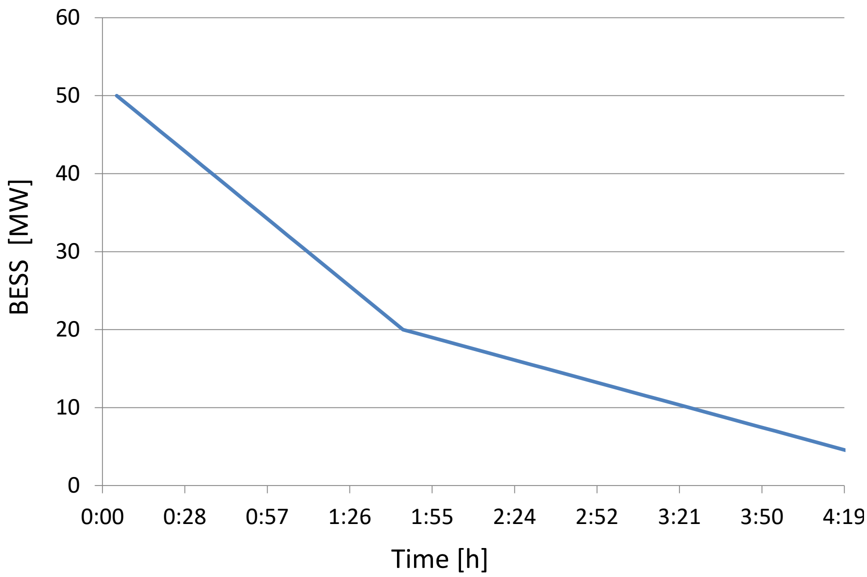

Figure 12. BESS resource output power.

Note that two relatively small storage resources of 50 [MW] each with a discharge rate of 1 and 0.5 [MW/h], respectively, accelerate the restoration times for both non-conventional and NCRES resources. This acceleration in the start-up of generation resources translates into a reduction in the time to reestablish the non-attended demand.

4.6. Inertia of the System

Figure 13 shows the accumulated inertia due to the number of synchronized generation units in the system. It is observed that the accumulated inertia curves for the first two scenarios are the same; this is because in both cases generators are synchronized at the same time. Likewise, due to the fact that starting times are accelerated with the integration of BESS, the inertia of the system increases in a shorter time, which allows the NCRES units a faster synchronization and therefore the non-served load decreases in less time. Figure 13 also shows that after 5 min, the minimum inertia criterion is already met and NCRES units can participate in the restoration process.

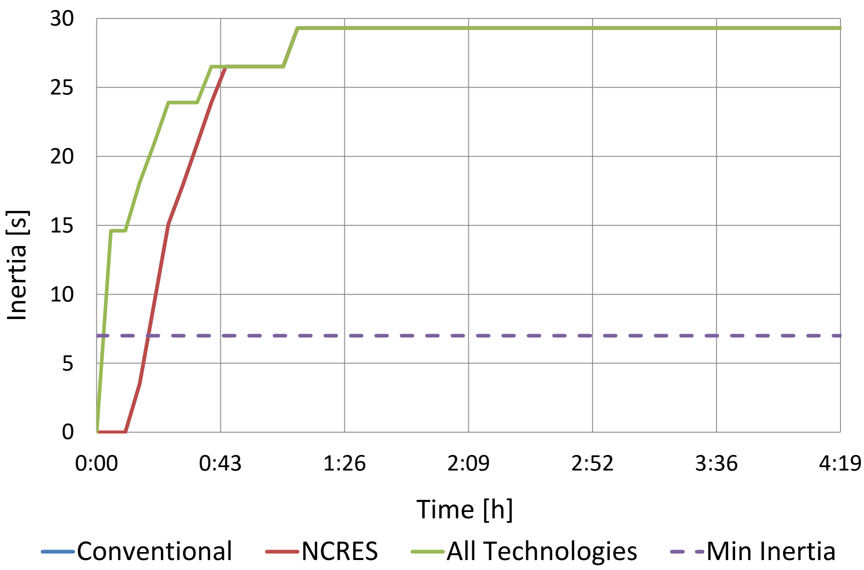

Figure 13. Cumulative inertia of the system.

5. Conclusions

This paper presented a mixed integer linear programming model to solve the optimal generation start-up problem integrating non-conventional renewable energy sources and battery energy storage systems. The proposed model considers different technical characteristics of the generating units and allows finding the optimal starting sequence of the generators in a power system after a blackout. The nature of the proposed model leads to global optimal solutions, clearly outperforming heuristic approaches. The objective function simultaneously minimizes the start-up times of the generating units and the energy not supplied to the system. The problem formulation uses rigorous mathematical modeling that simultaneously takes into account the critical start-up times of the units, the starting power requirements, and the load-generation balance of the system.

The numerical results obtained with the IEEE-39 RTS test system show the effectiveness and robustness of the proposed model as well as the benefits brought about by non-conventional renewable energy sources and battery energy storage systems. In particular, the results allow concluding that the inclusion of these technologies significantly improve the restoration time. Furthermore, the proposed approach can be implemented in real applications. This conclusion is based on the fact that the model guarantees a global optimal solution in fast execution time; therefore, it can be used as an initial road map for the system operator, indicating the order to follow in starting up generation resources in a way that it guarantees a fast and safe restoration process.

Author Contributions: Conceptualization, R.A.P.-M. and J.M.L.-L.; Data curation, R.A.P.-M.; Formal analysis, R.A.P.-M., N.M.-G., and J.M.L.-L.; Funding acquisition, J.M.L.-L. and N.M.-G.; Investigation, R.A.P.-M., N.M.-G., and J.M.L.-L.; Methodology, R.A.P.-M.; Project administration, R.A.P.-M., N.M.-G., and J.M.L.-L.; Resources, R.A.P.-M., N.M.-G., and J.M.L.-L.; Software, R.A.P.-M.; Supervision, N.M.-G. and J.M.L.-L.; Validation, R.A.P.-M., N.M.-G., and J.M.L.-L.; Visualization, R.A.P.-M., N.M.-G., and J.M.L.-L.; Writing—original draft, R.A.P.-M.; Writing—review and editing, R.A.P.-M., N.M.-G., and J.M.L.-L. All authors have read and agreed to the published version of the manuscript.

Funding: This research was funded by the Colombia Scientific Program within the framework of the so-called Ecosistema Científico (Contract No. FP44842-218-2018).

Institutional Review Board Statement: Not applicable.

Informed Consent Statement: Not applicable.

Data Availability Statement: Not applicable.

Acknowledgments: The authors gratefully acknowledge the support from the Colombia Scientific Program within the framework of the call Ecosistema Científico (Contract No. FP44842-218-2018). The authors also want to acknowledge Universidad de Antioquia for its support through the project "estrategia de sostenibilidad".

Conflicts of Interest: The authors declare that they have no conflict of interest.

The nomenclature used through the paper is provided here for quick reference:

Indexes	
i	Index of total generators, 1 to N; where N is a integer number
j	Index of NBS generators, 1 to M; where M is a integer number
k	Index of BS generators, 1 to N-M
l	Index of load unserved, 1 to L; where L is a integer number
rv	Index of NCRES, 1 to RV; where RV is a integer number
b	Index of BESS, 1 to B; where B is a integer number
t	Index of time intervals, 1 to T; where T is a integer number
h	Index of binary variables, 1 to 3
tr	Index of piecewise curves models, 1 to 5
Parameters	
T_{jcmax}	Critical maximum time interval in [h]
T_{jcmin}	Critical minimum time interval in [h]
T_{ictp}	Cranking time for NBS generators to begin to ramp up in [h]
R_{ri}	Generator ramping rate in [MW/h]
H_i	Generator Inertia in [h]
P_{jstart}	Generator start-up power requirement in [MW]
P_{imax}	Maximum generator active power output in [MW]
P_{lcarga}	Active power load in [MW]
$P_{rvstart}$	NCRES start-up power requirement in [MW]
P^t_{rvrt}	NCRES forecast active power in [MW]
$\overline{P}_{rvhistmed}$	NCRES historical average active power of previous week of blackout in [MW]
$\overline{P}_{rvforec}$	NCRES forecast average active power of previous week of blackout in [MW]
$p(v)_{rvhist}$	NCRES probability respect to NCRES historical average active power
$p(v)_{rvforec}$	NCRES probability respect to NCRES forecast average active power
$Hmin_{sys}$	Minimum inertia of the system that guarantees the stability in [h]
SOC_b	Initial state of charge BESS in [MW]
$SOCmin_b$	State of charge minimum of BESS in [MW]
$SOCmax_b$	State of charge maximum of BESS in [MW]
η_s	Ramping rate of BESS in [MW/h]
T	Total restoration time in [h]
t_{kstart}	BS start up time. It is equal to 0
t_{bON}	BESS start up time. It is equal to 0
$BigM$	Upper positive bound. It is equal to 9999

Variables

$Egen_{sys}$	Sum of MW capabilities minus start-up power requirements in [MW]
t_{jstart}	NBS generator starting time in [h]
t_{lrest}	load restoring time in [h]
$t_{rvstart}$	NCRES starting time in [h]
t_{itr}	Capability curve interval time in [h]
w_{ih}	Capability curve binary variable
w_{rvprob}	Binary decision variable of NCRES Start up probability
w_{rvH}	Binary decision variable of NCRES inertia
w_{rvH}	Binary decision variable of NCRES start-up power requirement
$v1_{rv}$,$v2_{rv}$	Artificial binary decision variables
y_{ih}	Artificial integer variable

References

1. Lindenmeyer, D.; Dommel, H.W.; Adibi, M.M. Power system restoration—A bibliographical survey. *Int. J. Electr. Power Energy Syst.* **2001**, *23*, 219–227. [CrossRef]
2. Allen, E.H.; Stuart, R.B.; Wiedman, T.E. No Light in August: Power System Restoration Following the 2003 North American Blackout. *IEEE Power Energy Mag.* **2014**, *12*, 24–33. [CrossRef]
3. Li, C.; Sun, Y.; Chen, X. Analysis of the blackout in Europe on November 4, 2006. In Proceedings of the 2007 International Power Engineering Conference (IPEC 2007), Singapore, 3–6 December 2007; pp. 939–944.
4. Ruiz, C.A.; Orrego, N.J.; Gutierrez, J.F. The Colombian 2007 black out. In Proceedings of the 2008 IEEE/PES Transmission and Distribution Conference and Exposition: Latin America, Bogota, Columbia, 13–15 August 2008; IEEE: Piscataway, NJ, USA; pp. 1–5.
5. Lai, L.L.; Zhang, H.T.; Lai, C.S.; Xu, F.Y.; Mishra, S. Investigation on July 2012 Indian blackout. In Proceedings of the 2013 International Conference on Machine Learning and Cybernetics, Tianjin, China, 14–17 July 2013; IEEE: Piscataway, NJ, USA, 2013; Volume 1, pp. 92–97.
6. Wu, Y.K.; Chang, S.M.; Hu, Y.L. Literature Review of Power System Blackouts. *Energy Procedia* **2017**, *141*, 428–431. [CrossRef]
7. Borghetti, A.; Nucci, C.A.; Paolone, M. Restoration Processes after Blackouts. In *Handbook of Electrical Power System Dynamics: Modeling, Stability, and Control*; John Wiley Sons: Hoboken, NJ, USA, 2013; pp. 864–899. [CrossRef]
8. Sun, W.; Liu, C.C.; Liu, S. Black Start Capability Assessment in Power System Restoration. In Proceedings of the 2011 IEEE Power and Energy Society General Meeting, Detroit, MI, USA, 24–29 July 2011; IEEE: Piscataway, NJ, USA, 2011; pp. 1–7. [CrossRef]
9. Ketabi, A.; Karimizadeh, A.; Shahidehpour, M. Optimal generation units start-up sequence during restoration of power system considering network reliability using bi-level optimization. *Int. J. Electr. Power Energy Syst.* **2019**, *104*, 772–783. [CrossRef]
10. Shen, C.; Kaufmann, P.; Braun, M. Optimizing the generator start-up sequence after a power system blackout. In Proceedings of the IEEE Power and Energy Society General Meeting, National Harbor, MD, USA, 27–31 July 2014; pp. 1–5. [CrossRef]
11. Ketabi, A.; Feuillet, R. Ant Colony Search Algorithm for Optimal Generators Startup during Power System Restoration. *Math. Probl. Eng.* **2010**, *2010*, 906935. [CrossRef]
12. El-Zonkoly, A.M. Renewable energy sources for complete optimal power system black-start restoration. *IET Gener. Transm. Distrib.* **2015**, *9*, 531–539. [CrossRef]
13. Gu, X.; Liu, W.; Sun, C. Optimisation for unit restarting sequence considering decreasing trend of unit start-up efficiency after a power system blackout. *IET Gener. Transm. Distrib.* **2016**, *10*, 4187–4196. [CrossRef]
14. Gu, X.; Zhong, H. Optimisation of network reconfiguration based on a two-layer unit-restarting framework for power system restoration. *IET Gener. Transm. Distrib.* **2012**, *6*, 693–700. [CrossRef]
15. Urrea, R.; Gomez, J. Modelo Experto Para Apoyo en Restablecimiento de Sistemas de Potencia. In Proceedings of the XIII Eriac Cigre meeting, Puerto Iguazú, Argentina, 24–28 May 2009; Cigré: Puerto Iguazú, Argentina, 2009; pp. 1–9.
16. Zhong, H.R.; Gu, X.P. Determination of optimal unit start-up sequences based on fuzzy AHP in power system restoration. In Proceedings of the 2011 4th International Conference on Electric Utility Deregulation and Restructuring and Power Technologies (DRPT), Weihai, China, 6–9 July 2011; pp. 1541–1545. [CrossRef]
17. Sun, L.; Lin, Z.; Xu, Y.; Wen, F.; Zhang, C.; Xue, Y. Optimal Skeleton-Network Restoration Considering Generator Start-Up Sequence and Load Pickup. *IEEE Trans. Smart Grid* **2019**, *10*, 3174–3185. [CrossRef]
18. Zhao, Y.; Lin, Z.; Ding, Y.; Liu, Y.; Sun, L.; Yan, Y. A Model Predictive Control Based Generator Start-Up Optimization Strategy for Restoration with Microgrids as Black-Start Resources. *IEEE Trans. Power Syst.* **2018**, *33*, 7189–7203. [CrossRef]
19. Zhao, J.; Zhang, Q.; LIU, Z.; WU, X. A Distributed Black-Start Optimization Method for Global Transmission and Distribution Network. *IEEE Trans. Power Syst.* **2021**, *36*, 4471–4481. [CrossRef]
20. Hu, R.; Hu, W.; Li, P.; Su, C.; Chen, Z. A Dynamic Programming based Method for Optimizing Power System Restoration with High Wind Power Penetration. In Proceedings of the 2016 IEEE 8th International Power Electronics and Motion Control Conference(IPEMC-ECCE Asia), Hefei, China, 22–26 May 2016; pp. 2022–2027. [CrossRef]

21. Sun, W.; Liu, C.C. Optimal transmission path search in power system restoration. In Proceedings of the IREP Symposium: Bulk Power System Dynamics and Control—IX Optimization, Security and Control of the Emerging Power Grid, IREP 2013, Rethymno, Greece, 25–30 August 2013; pp. 1–5. [CrossRef]
22. Zhao, B.; Dong, X.; Bornemann, J. Service Restoration for a Renewable-Powered Microgrid in Unscheduled Island Mode. *IEEE Trans. Smart Grid* **2015**, *6*, 1128–1136. [CrossRef]
23. Correa Posada, C.M. Modelo de Optimización para las Plantas térmicas de Generación de ciclo Combinado en el Despacho Económico. Master's Thesis, Universidad Nacional de Colombia, Bogotá, Colombia, 2009.
24. Yao, F.; Chau, T.K.; Zhang, X.; Iu, H.H.C.; Fernando, T. An Integrated Transmission Expansion and Sectionalizing-Based Black Start Allocation of BESS Planning Strategy for Enhanced Power Grid Resilience. *IEEE Access* **2020**, *8*, 148968–148979. [CrossRef]
25. Zhang, B.; Dehghanian, P.; Kezunovic, M. Optimal Allocation of PV Generation and Battery Storage for Enhanced Resilience. *IEEE Trans. Smart Grid* **2019**, *10*, 535–545. [CrossRef]
26. Sprooten, J.; Gunst, T.; Mestdag, C.; Bronckart, O. Power system restoration with high penetration level of renewable generation—New challenges and strategies. In Proceedings of the 2014 Saudi Arabia Smart Grid Conference (SASG), Jeddah, Saudi Arabia, 14–17 December 2014; IEEE: Piscataway, NJ, USA, 2014; pp. 1–8. [CrossRef]
27. Li, J.; Ma, X.Y.; Liu, C.C.; Schneider, K.P. Distribution System Restoration with Microgrids Using Spanning Tree Search. *IEEE Trans. Power Syst.* **2014**, *29*, 3021–3029. [CrossRef]
28. Singh, S.; Fozdar, M.; Malik, H.; Fernández Moreno, M.d.V.; García Márquez, F.P. Influence of Wind Power on Modeling of Bidding Strategy in a Promising Power Market with a Modified Gravitational Search Algorithm. *Appl. Sci.* **2021**, *11*, 4438. [CrossRef]
29. Liu, C.C.; Liou, K.L.; Chu, R.; Holen, A. Generation capability dispatch for bulk power system restoration: A knowledge-based approach. *IEEE Trans. Power Syst.* **1993**, *8*, 316–325. [CrossRef]
30. El-Zonkoy, A. Integration of wind power for optimal power system black-start restoration. *Turk. J. Electr. Eng. Comput. Sci.* **2015**, *23*, 1853–1866. [CrossRef]
31. Sun, W.; Liu, C.C.; Zhang, L. Optimal generator start-up strategy for bulk power system restoration. *IEEE Trans. Power Syst.* **2011**, *26*, 1357–1366. [CrossRef]
32. System Optimization Techniques. Available online: https://pascua.iit.comillas.edu/aramos/TOS.htm (accessed on 27 August 2021).
33. Ordoudis, C.; Pinson, P.; Morales-González, J.M.; Zugno, M. *An Updated Version of the IEEE RTS 24-Bus System for Electricity Market and Power System Operation Studies*; Technical University of Denmark (DTU): Lyngby, Denmark, 2016.
34. Elia Group, TSO. 2020. Available online: https://www.elia.be/en/grid-data/power-generation (accessed on 27 August 2021).